J. Mater. Environ. Sci. 7 (11) (2016) 4311-4323
ISSN : 2028-2508
CODEN: JMESCN

Corrosion protection of mild steel by 6-chloroquinoxaline-2,3(1H,4H)-dione as a new inhibitor in hydrochloric acid solution

A. El Janati[1], Y. Kandri Rodi[1], H. Elmsellem[2]*, F. Ouazzani Chahdi[1], A. Aouniti[2], B. El Mahi[2], Y. Ouzidan[1], N. K. Sebbar[3], E. M. Essassi[3,4]

[1]Laboratoire de Chimie Organique Appliquee, Université Sidi Mohamed Ben Abdallah, Faculté des Sciences et Techniques, Route d'Immouzzer, BP 2202 Fes, Morocco.
[2] Laboratoire de chimie analytique appliquée, matériaux et environnement (LC2AME), Faculté des Sciences, B.P. 717, 60000 Oujda, Morocco.
[3]Laboratoire de Chimie Organique Hétérocyclique, URAC 21, Pôle de Compétences Pharmacochimie, Mohammed V University in Rabat, Faculté des Sciences, Av. Ibn Battouta, BP 1014 Rabat, Morocco.
[4]Moroccan Foundation for Advanced Science, Innovation and Research (MASCIR), Rabat Design Center, Rue Mohamed Al Jazouli, Madinat El Irfane, Rabat, Morocco.

Received 17 June 2016, Revised 20 Sept 2016, Accepted 24 Sept 2016
**Corresponding author. E-mail: h.elmsellem@yahoo.fr; Tél: +212670923431/+212600254809*

Abstract

In the present study, the effectiveness of 6-chloroquinoxaline-2,3(1H,4H)-dione (P2) on the corrosion inhibition of mild steel in 1 mol L-1 HCl has been analyzed using weight loss measurements, potentiodynamic polarization, electrochemical impedance spectroscopy and quantum chemical study(DFT). This organic inhibitor was characterized by FT-IR, and thermodynamic parameters were calculated. The polarization showed that the inhibition efficiency of compound **(P2)** was increased with increasing the concentration of P2. The electronic properties obtained using quantum chemical approach was correlated with the experimental inhibition efficiencies.

Keywords: Mild steel, 6-chloroquinoxaline-2,3(1H,4H)-dione, EIS, Corrosion, Weight loss, Electrochemical, DFT

1. Introduction

Mild steel is an iron-containing alloy, considered as one of important constructional materials extensively used in different applications. Generally, acid solution (especially HCl) plays a significant role in many fields of industry such as pickling, descaling and oil well acidification, its price is generally low and more consistent [1,2]. The cost of managing/cleaning spills is usually much that most industries would rather device means to prevent corrosion. Also, the down time due to shut down of plant for maintenance and damage to employee or company integrity is undesirable. Therefore, huge amounts are spent on corrosion inhibitors, being a simple, practical and cost effective means of reducing corrosion. Corrosion inhibitors are therefore an important class of oilfield chemicals, like surfactants, mud additives, scale inhibitors, biocides, etc. Corrosion inhibitors are substances which are added in small amounts to the aggressive fluid in order to retard the speed of corrosive attack on the metal surface it contacts [3]. Even recently, many compounds that contain functionalities like nitrogen, oxygen, multiple bonds, conjugated double bond systems, heteroatoms and aromatic rings have been found to be efficient for different metals in various media [4–6]. The corrosion inhibition of a metal may involve either physisorption or chemisorption of the inhibitor on the metal surface. Electrostatic attraction

between the charged hydrophilic groups and the charged active centers on the metal surface leads to physicosorption. Several authors showed that most inhibitors were adsorbed on the metal surface by displacing water molecules from the surface and forming a compact barrier film [7]. The choice of an optimal inhibitor should be based on three considerations: *(i)* it should have a convenient synthesis from inexpensive raw materials, *(ii)* the presence of phosphorus, nitrogen, oxygen, sulfur and multiple bonds in the inhibitor molecule are required for its efficiency and *(iii)* its toxicity toward the environment must be negligible [8].

Recently, in addition to experimental investigations, the evaluation of inhibition performance is also conducted theoretically by DFT calculation studies for the understanding of some experimentally unknown properties, exploring and establishing relationships between inhibitor molecules and the metal surface [9, 10].

Over the years, Quinoxaline derivatives are a versatile class of nitrogen containing heterocyclic compounds and they constitute useful intermediates in organic synthesis and medicinal chemistry. They possess a broad spectrum of biological activities including anti-bacterial, [11] anti-inflammatory, [12] anticancer, [13] and kinase inhibitors.[14] In addition, quinoxaline derivatives have been evaluated as anthelmintic agents, semiconductors, dyes and biocides [15, 16].

On continuation of our works related to the use of new organic inhibitors [17- 21], the present study reports on the effect of 6-chloroquinoxaline-2,3(1H,4H)-dione (P2) (Figure 1) for inhibition of mild steel corrosion in 1 mol L^{-1} HCl.

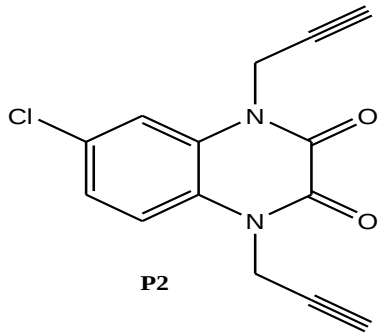

Figure 1. 6-chloroquinoxaline-2,3(1H,4H)-dione (**P2**)

2. Experimental

2.1. Materials and solutions

The mild steel of the composition 0.07 wt. % C, 0.008 wt.% P, 0.34 wt.% Mn, remaining iron (Fe) was used in the study. The metal specimens used for weight loss measurements were cut to obtain rectangular surfaces with dimensions of 1.5 x 1.5 x 0.05 cm3 with a hole drilled at the upper edge in order to hook them to a glass rod and immerse in the aggressive medium. Substantial layer of the specimen was removed by using various grades of abrasive papers and degreased by scrubbing with bleach-free scouring powder, followed by thorough rinsing in water and acetone. Mild steel corrosion behavior in 1 M HCl was investigated in the absence and the presence of quinoxaline derivative (P2) with the help of weight loss and electrochemical techniques. It was seen that mild steel dissolution rate was very high in 1 M HCl alone but presence of inhibitor significantly decreased the corrosion rate of mild steel. The acid solutions (1.0 M HCl) were prepared by dilution of analytical reagent-grade 98 % HCl with double-distilled water. The range of concentration of P2 was 10-6 M to 10-3 M.

2.2. Synthesis of inhibitor

To a solution of 6-chloroquinoxaline-2,3(1H,4H)-dione in 20 ml of DMF, potassium carbonate (1.2 eq), tetra n-butylammonium bromide (TBAB) (0.1 eq) was added propargyl bromide (2.5 eq). Stirring was continued at room temperature for 6 hours. After removing salts by filtration, the DMF was evaporated under reduced pressure and the residue obtained is dissolved in dichloromethane. The remaining salts are extracted with distilled water and the resulting mixture was chromatographed on silica gel column (eluent: ethyl acetate/hexane (1/3)). The product was obtained with 82 % yield. (**Schema 1**):

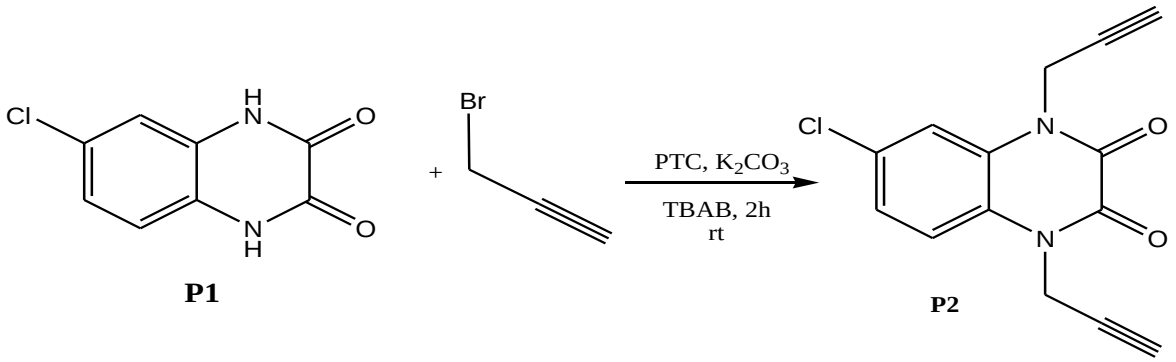

Scheme 1. Synthesis of 6-chloroquinoxaline-2,3(1H,4H)-dione (**P2**).

The analytical and spectroscopic data are conforming to the structure of compound formed:

(P2): Yield: 82%; **RMN^{1}H (DMSO-d6) δ ppm:** 7.58(d,1H,H_{Ar},J=2.4Hz); 7.51(d,1H,H_{Ar},J=8.9Hz); 7.42(dd,1H,H_{Ar},J=8.8Hz); 5.01(d,2H,CH_2,J=2.4Hz); 4.97(d,2H,CH_2,J=2.4Hz); 3.38(2T,C≡CH,J=2.4Hz). **RMN^{13}C (DMSO-d6) δ ppm:** 153.35, 153.15(C=O); 128.67, 127.51, 125.40(Cq); 124.12, 117.75, 115.92(CH_{Ar}); 78.05, 78.03(C≡CH); 76.12, 76.06(C≡CH); 32.91, 32.82(CH_2).

2.3. Electrochemical measurements

The electrochemical study was carried out using a potentiostat PGZ100 piloted by Voltamaster soft-ware. This potentiostat is connected to a cell with three electrode thermostats with double wall. A saturated calomel electrode (SCE) and platinum electrode were used as reference and auxiliary electrodes, respectively. Before all experiments, the potential was stabilized at free potential during 30 min. The solution test is there after de-aerated by bubbling nitrogen. The electrochemical impedance spectroscopy (EIS) measurements are carried out with the electrochemical system, which included a digital potentiostat model Voltalab PGZ100 computer at Ecorr after immersion in solution without bubbling. After the determination of steady-state current at a corrosion potential, sine wave voltage (10 mV) peak to peak, at frequencies between 100 kHz and 10 mHz are superimposed on the rest potential. Computer programs automatically controlled the measurements performed at rest potentials after 0.5 hour of exposure at 308 K. The impedance diagrams are given in the Nyquist representation. Experiments are repeated three times to ensure the reproducibility.

2.4. Quantum chemical calculations

Quantum chemical calculations are used to correlate experimental data for inhibitors obtained from different techniques (viz., electrochemical and weight loss) and their structural and electronic properties. According to Koop man's theorem [22], E_{HOMO} and E_{LUMO} of the inhibitor molecule are related to the ionization potential (I) and the electron affinity (A), respectively. The ionization potential and the electron affinity are defined as $I = -E_{HOMO}$ and $A = -E_{LUMO}$, respectively. Then absolute electronegativity (χ) and global hardness (η) of the inhibitor molecule are approximated as follows [23]:

$$\chi = \frac{I+A}{2} \ , \ \chi = -\frac{1}{2}(E_{HOMO} + E_{LUMO}) \textbf{ (1)}$$

$$\eta = \frac{I-A}{2} \ , \ \eta = -\frac{1}{2}(E_{HOMO} - E_{LUMO}) \textbf{ (2)}$$

Where $I = -E_{HOMO}$ and $A = -E_{LUMO}$ are the ionization potential and electron affinity respectively.
The fraction of transferred electrons ΔN was calculated according to Pearson theory [24]. This parameter evaluates the electronic flow in a reaction of two systems with different electronegativities, in particular case; a metallic surface (Fe) and an inhibitor molecule. ΔN is given as follows:

$$\Delta N = \frac{\chi_{Fe} - \chi_{inh}}{2(\eta_{Fe} + \eta_{inh})} \textbf{ (3)}$$

Where χFe and χinh denote the absolute electronegativity of an iron atom (Fe) and the inhibitor molecule, respectively; ηFe and ηinh denote the absolute hardness of Fe atom and the inhibitor molecule, respectively. In order to apply the eq. 3 in the present study, a theoretical value for the electronegativity of bulk iron was used χFe = 7 eV and a global hardness of ηFe = 0, by assuming that for a metallic bulk I = A because they are softer than the neutral metallic atoms [25, 26].
The electrophilicity has been introduced by Sastri et al. [23], is a descriptor of reactivity that allows a quantitative classification of the global electrophilic nature of a compound within a relative scale. They have proposed the ω as a measure of energy lowering owing to maximal electron flow between donor and acceptor and ω is defined as follows.

$$\omega = \frac{\chi^2}{2\eta} \textbf{(4)}$$

The Softness σ is defined as the inverse of the η [26]

$$\sigma = \frac{1}{\eta} \textbf{(5)}$$

3. Results and discussion

3.1. Weight loss measurements

3.1.1. Corrosion inhibition performance of P2

The corrosion of mild steel in 1 mol L^{-1} HCl in the absence and presence of various concentrations (10^{-6} to 10^{-3} M) of P2 was investigated at temperature 308K using weight loss measurements for 6 h immersion period. Corrosion rate (*v*), inhibition efficiency (E_w%) and surface coverage (θ) were calculated using the Eqs. (6) – (7) and the results are given in Table 1. The average weight loss was obtained. The corrosion rate (*v*) is calculated using the following equation:

$$v = \frac{w}{st} \textbf{(6)}$$

Where: W is the average weight loss, S the total area, and t is immersion time. With the corrosion rate calculated, the inhibition efficiency (E_w) is determined as follows:

$$Ew\ \% = \frac{v_0 - v}{v_0} X\ 100 \textbf{(7)}$$

Where: v_0 and *v* are, respectively, the values of corrosion rate with and without inhibitor.

Table 1 Corrosion parameters for various concentrations of P2 on mild steel in 1 M HCl.

Inhibitor	**Concentration** (M)	***v*** ($mg.cm^{-2}\ h^{-1}$)	**E_w** (%)
1M HCl	--	0.82	--
P2	**10^{-6}**	0.31	62
	10^{-5}	0.19	77
	10^{-4}	0.12	85
	10^{-3}	0.08	90

Analysis of Table 1 clearly indicates that the rate of corrosion on the mild steel surface in the presence of P2 was found to be dependent on up to 10^{-3} concentration of P2. Beyond this concentration, there is no appreciable change in the inhibiting performance of P2, indicating the attainment of limiting value.
The increased inhibition efficiency with an increase in P2 concentration indicates that more P2 molecules are adsorbed on the steel surface leading to the formation of a protective film [27].
This behavior could be attributed to the increase in the surface coverage by the adsorption of inhibitor on the mild steel surface, which trims down the contact between the mild steel surface and acidic medium, thereby reducing the corrosion process [28, 29]. The adsorption of P2 may be attributed to the interaction between the lone pair of electrons of O; N atoms and the vacant d orbitals of iron atom of the mild steel surface. However,

the presence of chloride ions in the hydrochloric acid solution containing P2 plays a significant role in the adsorption process that results from an increased surface coverage as a result of ion-pair interactions between the organic cat ions and the chloride ions [30, 31].

3.2. Adsorption isotherm

It is evident that the corrosion inhibition process is based on the adsorption of the inhibitor molecules on the metallic surface. Generally, two modes of adsorption can be considered.
Physical adsorption requires the presence of electrically charged metal surface and charged species in the bulk of the solution. The second mode is the chemisorption which requires charge sharing or charge transfer from the inhibitor molecule to the metal surface. In order to specify the adsorption mode of 6-chloroquinoxaline-2,3(1H,4H)-dione (P2) molecule on the mild steel electrode surface in the HCl solution, the degree of surface coverage, θ, at different concentrations of the inhibitor in the stagnant naturally aerated neutral chloride solution was determined from the corresponding gravimetric measurements according to:

$$\theta = E_w/100 \qquad \textbf{(8)}$$

The obtained values of θ were fitted to different isotherms including Langmuir, Frumkin and Temkin isotherms. The best fitting was found to obey the Langmuir adsorption isotherm,
Eq. (9), which is based on the assumption that all adsorption sites are equivalent and that particle binding occurs independently from nearby sites being occupied or not [32, 33]:

$$KC=\theta/(1-\theta) \qquad \textbf{(9)}$$

where C is the concentration of inhibitor, θ, the fractional surface coverage and K is the adsorption equilibrium constant related to the free energy of adsorption ΔG_{ads} as [34]:

$$\Delta G_{ads} = -RT\ln(K \times C_{solvent}) \qquad \textbf{(10)}$$

where $C_{solvent}$ represents the molar concentration of the solvent. In the case of water Csolvent is 55.5 mol dm^{-3}, R the universal gas constant and T is the absolute temperature. Eq. (11) can be rearranged to obtain the following formulation:

$$\frac{C}{\theta} = \frac{1}{k} + C \qquad \textbf{(11)}$$

A plot of C/θ as a function of C gives a straight line with a slope of unity. Such linear relationship was verified for the adsorption of P2 on the electrode surface (Figure 2).
The free energy of adsorption, ΔG_{ads} , was calculated and found to be equal to -42.88 kJ mol^{-1}. A value of -40 kJ mol^{-1} is usually adopted as a threshold value between chemisorption and physisorption [34, 35]. Therefore the adsorption of the investigated inhibitor molecules on mild steel electrode is of a chemical nature.

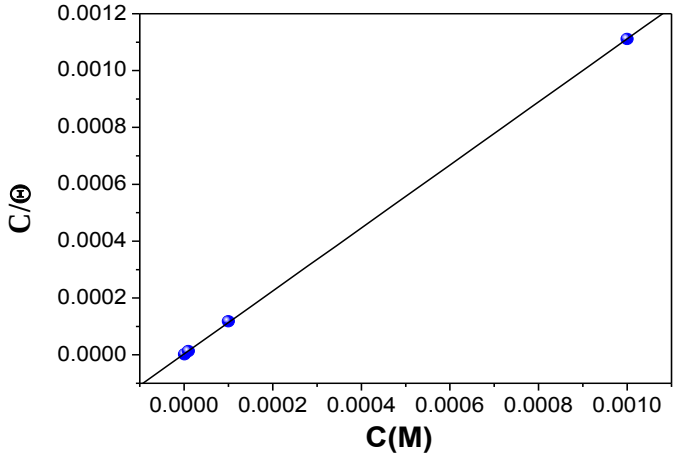

Figure 2. Langmuir isotherms of the adsorption P2 on the mild steel surface in 1 M HCl solution at 308K.

3.3. Potentiodynamic polarization measurements

Polarization measurements were carried out in order to gain knowledge concerning the kinetics of the cathodic and anodic reactions. Figure 3 shows the cathodic and anodic polarization curves of mild steel immersed in HCl in the absence and presence of different concentrations of the inhibitor P2.
Electrochemical parameters such as corrosion potential (E_{corr}), corrosion current density (i_{corr}), cathodic and anodic Tafel slopes (βc) were calculated. From the obtained polarization curves, it is clear that the corrosion current densities (i_{corr}) were decreased with increasing concentration of inhibitor P2 with respect to the blank (inhibitor free solution). These results confirm the formation of a good protective layer on the surface of mild steel. The percentage inhibition efficiency (E_p%) were calculated using the following equations [36]:

$$E_p\% = (i_{corr(0)} - i_{corr(inh)} / i_{corr(0)}) * 100 \quad \textbf{(12)}$$

where $i_{corr(0)}$ and $i_{corr(inh)}$ represent corrosion current density values without and with inhibitor, respectively;

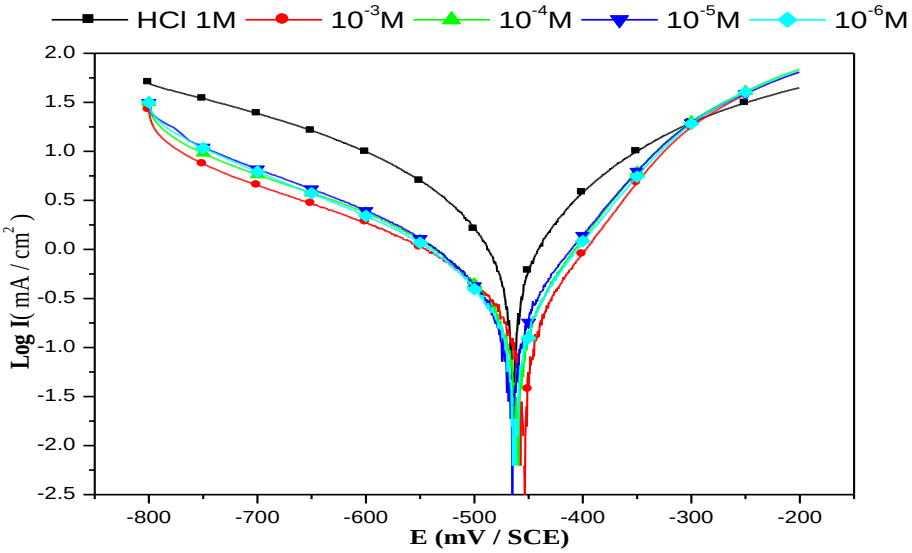

Figure 3. Polarisation curves of mild steel in 1M HCl at different concentrations of P2.

Table 2. Values of electrochemical parameters evaluated from the cathodic current-voltage characteristics for the system electrode/1 M HCl with and without added inhibitor at 308 K.

Inhibitor	**Concentration** (M)	**-E_{corr}** (mV/SCE)	**I_{corr}** (μA/cm^2)	**-βc** (mV dec^{-1})	**E_p** (%)
1M HCl	**-**	464	1386	184	--
P2	**10^{-6}**	462	514	177	63
	10^{-5}	469	357	193	74
	10^{-4}	461	201	168	85
	10^{-3}	455	155	172	89

From the obtained data, it is clear that Tafel lines are shifted to more negative and more positive potentials for the anodic and cathodic processes, respectively relative to the blank curve. This means that the selected compound acts as a mixed type inhibitor, i.e., promoting retardation of both anodic and cathodic discharge reactions.
The values of cathodic Tafel slope (βc) of P2 are found to change with inhibitor concentration, indicating that the inhibitor controlled both the reactions. In other words, the inhibitors decrease the surface area for corrosion

without affecting the mechanism of corrosion and only cause inactivation of a part of the surface with respect to the corrosive medium [37, 38].
Complete data obtained from polarization measurements are summarized and listed in Table 2. The results indicate the percentage inhibition efficiency (E_p%) of P2 could be attributed to the O and N of inhibitor molecules, which promotes stronger adsorbed film and hence more protective layer and higher inhibition efficiency. Also, it noticed that the corrosion inhibition enhances with increasing the inhibitor concentration. This behavior is due to the fact that the adsorption amount and coverage of inhibitor on mild steel surface increases with the inhibitor concentrations [39 , 40].

3.4. Electrochemical Impedance Spectroscopy (EIS)

The aim of these investigations was to determine the influence of *P2* on the electrochemical behaviour of mild steel in 1 M HCl. Polarisation curves of the mild steel electrode in 1 M HCl without and with addition of various concentrations of *P2* are shown in Figure 4. As it can be seen, the anodic and cathodic reactions are affected by the addition of *P2*. It is noted that this plot was composed for one capacitive loop in the absence and presence of *P2*, indicating that almost no change in the corrosion mechanism with the presence of *P2*. This behavior can be attributed to charge transfer of the corrosion process. It is also noted that the diameter of the semicircle increases with inhibitor concentration, indicating an increase in corrosion resistance of the material [41].
It allows employing *CPE* element in order to investigate the inhibitive film properties on metallic surface. Thus, the impedance of the *CPE* can be described by the following equation:

$$Z_{CPE}=[Q(jw)^n]^{-1} \qquad \textbf{(13)}$$

Where *j* is the imaginary number, *Q* is the frequency independent real constant, $\omega = 2\pi f$ is the angular frequency (rad s^{-1}), *f* is the frequency of the applied signal, *n* is the *CPE* exponent for whole number of *n* = 1, 0, -1, *CPE* is reduced to the classical lump element-capacitor (*C*), resistance (*R*) and inductance (*L*) [42]. The use of these parameters, similar to the constant phase element (*CPE*), allowed the depressed feature of Nyquist plot to be reproduced readily.
The inhibition efficiency of the inhibitor was calculated from the charge transfer resistance values using the following equation:

$$E\% = \frac{R_{ct} - R_{ct}^{\circ}}{R_{ct}} \times 100 \qquad \textbf{(14)}$$

Where, R°_{ct} and R_{ct} are the charge transfer resistance in absence and in presence of inhibitor, respectively.
The most important data obtained from the equivalent circuit are presented in Figure 4. It may be remarked that R_{ct} value increases and C_{dl} decreases with inhibitor concentration indicating that more inhibitor molecules are adsorbed on mild steel surface and provided better surface coverage and/or enhanced the thickness of the protective layer at the metal/solution interface [43, 44].
In addition, these change in R_{ct} and C_{dl} can be attributed to the gradual displacement of water molecules and/or chloride ions on the mild steel surface [45], leading to a protective solid film, then a decrease in the extent of dissolution reaction [46, 48]. In the other, the decrease of C_{dl} with concentration can be explained by the decrease in local dielectric constant and/or an increase in the protective layer thickness on the electrode surface. This trend is in accordance with Helmhotz model, given by the following equation [49]

$$C_{dc} = (\varepsilon_0 \varepsilon / e) \times S \qquad \textbf{(15)}$$

where ε is the dielectric constant of the protective layer, ε_0 is the permittivity of free space (8.854×10^{-14} Fcm^{-1}) and *S* is the effective surface area of the electrode.
However, the inhibition efficiencies obtained from electrochemical impedance measurements, increase with concentration and show the same trend as those obtained from potentiodynamic polarization and gravimetric measurements.
The results can be interpreted using equivalent circuit presented in *Figure 4*, which has been used previously to model the mild steel/acid interface [50, 52].
It is obvious from the results that the *P2* inhibits the corrosion of mild steel in 1 M HCl solution at all concentrations used in this study and the E(%) was seen to increase continuously with increasing additive

concentration at 308 K. Indeed, the protection efficiency increases with increasing of inhibitor concentration, the maximum E*(%)* of 90 % was achieved at 10^{-3}M.

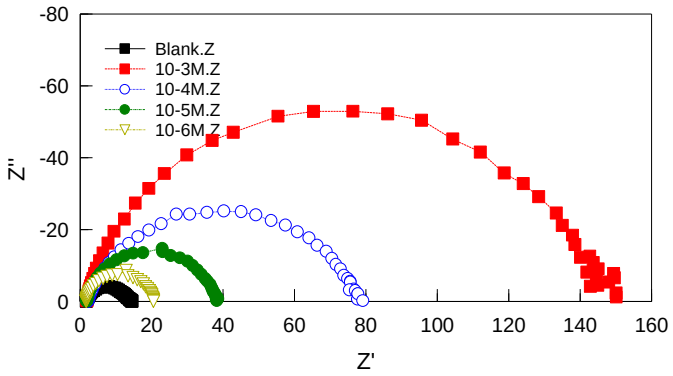

Figure 4. Nyquist diagram for mild steel in 1 M HCl solution in the absence and presence of different concentrations of **P2**.

From the respective phase angle Bode plots Figure 5, two phase maxima were present, the major one at lower frequencies and the other as a shoulder at intermediate frequencies, such behavior indicates the presence of two time constants representing the electrode processes. The phase maxima appearing in the low frequency range were attributed to the protective oxide film and the phase maximum at the intermediate frequency range corresponds to the electrical double layer.

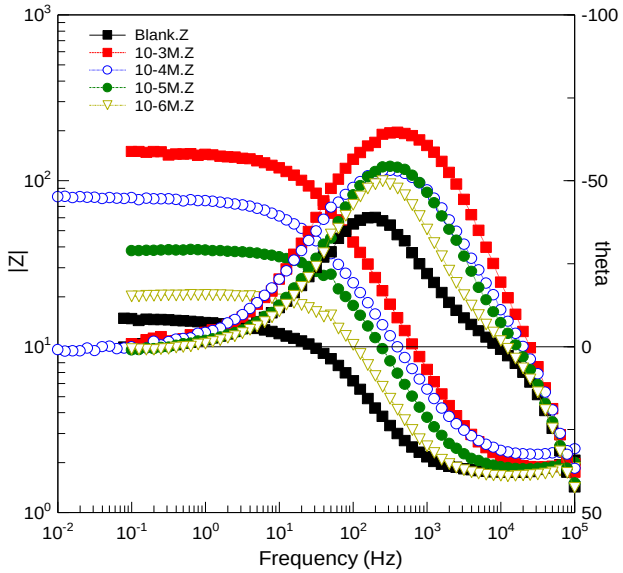

Figure 5. Bode and Phase angle plots of mild steel in 1 M HCl in the absence and presence of different concentrations of **(P2)** at 308K.

Figure 5. The Bode plots show resistive region at high frequencies and capacitive region at intermediate frequencies but do not show a clear resistive region (horizontal line and a phase angle at low frequencies (Figure 5). These plots show two overlapped phase maxima at intermediate and low frequencies. The Nyquist plots show a depressed semicircular shape with their centers below the real axis (Figure 6). This behavior is typical for solid metal electrodes that show frequency dispersion of the impedance data. The recorded resistance values increase with the increasing inhibitor concentration indicating that the electrode surface gets more protection. For a simple equivalent circuit Figure 7 consisting of a parallel combination of a CPE, and a resistor, Rct.

Table 3. Electrochemical parameters for mild steel in 1 M HCl without and with different concentrations of **(**P2**)** at 308K.

Concentration (M) / Prameters	**1M HCl**	**10^{-6}**	**10^{-5}**	**10^{-4}**	**10^{-3}**
Real Center	9.25	11.034	19.987	40.19	74.466
Imag. Center	1.62	1.8368	4.6551	16.125	24.047
Diameter	15.13	19.127	37.642	82.913	154.11
Deviation	0.15	0.18421	0.22762	0.488	1.4407
Low Intercept R_s ($\Omega.cm^2$)	1.86	1.6483	1.7513	1.9977	1.2569
High Intercept R_t ($\Omega.cm^2$)	16.64	20.419	38.224	78.382	147.67
Depression Angle	12.42	11.073	14.32	22.889	18.184
ω_{max} (rad s^{-1})	929.60	375.78	358.24	157.44	163.83
Estimated R_t($\Omega.cm^2$)	14.78	18.771	36.472	76.385	146.42
Estimated C_{dl}($F.cm^{-2}$)	7.11 E-5	6.1391E-5	5.4157E-5	4.6604E-5	3.9607E-5
E (%)	--	21	59	81	**90**

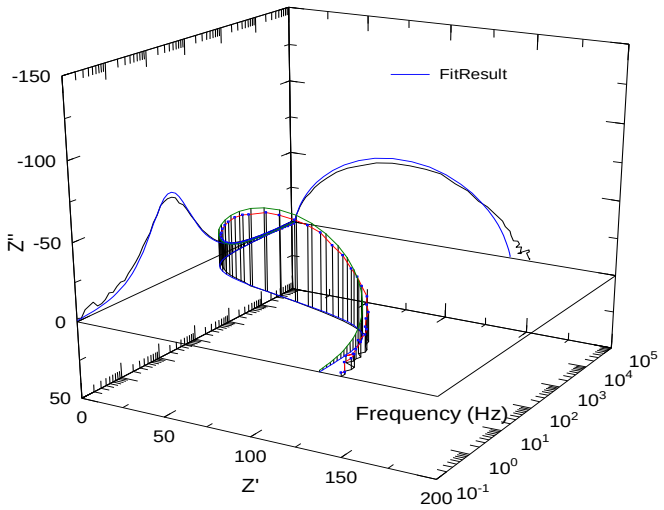

Figure 6. EIS Nyquist and Bode diagrams 3D for mild steel/1 M HCl + 10^{-3} M of **P2** interface: (------) experimental; (------) fitted data.

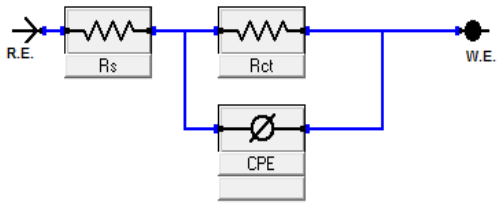

Figure 7. Equivalent circuit model used to fit the impedance spectra.

3.5. Computational theoretical studies

In the last few years, the FMOs (HOMO and LUMO) are widely used for describing chemical reactivity. The HOMO containing electrons, represents the ability (E_{HOMO}) to donate an electron, whereas, LUMO haven't not electrons, as an electron acceptor represents the ability (E_{LUMO}) to obtain an electron. The energy gap between HOMO and LUMO determines the kinetic stability, chemical reactivity, optical polarizability and chemical hardness–softness of a compound [53].

In this paper, we calculated the HOMO and LUMO orbital energies by using B3LYP method with 6-31G. All other calculations were performed using the results with some assumptions. The higher values of E_{HOMO} indicate an increase for the electron donor and this means a better inhibitory activity with increasing adsorption of the inhibitor on a metal surface, whereas E_{LUMO} indicates the ability to accept electron of the molecule. The adsorption ability of the inhibitor to the metal surface increases with increasing of E_{HOMO} and decreasing of E_{LUMO}.
High ionization energy (I= 7.06 eV, I= 7.46 eV in gas and aqueous phases respectively) indicates high stability [54, 56], the number of electrons transferred (ΔN) was also calculated and tabulated in Table 4. The number of electrons transferred (ΔN) was also calculated and tabulated in Table 4. The ΔN(gas) < 3.6 and ΔN(aqueous) < 3.6 indicates the tendency of a molecule to donate electrons to the metal surface [57, 58].

Table 4. Quantum chemical descriptors of the studied inhibitor at B3LYP/6-31G in gas, G and aqueous, A phases.

Prameters	Phase	
	Gas	Aqueous
Total Energy *TE* (eV)	-34255.7	-34249.2
E_{HOMO} (eV)	-7.0615	-7.4645
E_{LUMO} (eV)	-0.1170	-1.2435
Gap ΔE (eV)	6.9445	6.2210
Dipole moment μ (Debye)	4.0157	6.4467
Ionisation potential I (eV)	7.0615	7.4645
Electron affinity A	0.1170	1.2435
Electronegativity χ	3.5893	4.3540
Hardness η	3.4723	3.1105
Electrophilicity index ω	1.8551	3.0473
Softness σ	0.2880	0.3215
Fractions of electron transferred ΔN	0.4911	0.4253

The geometry of P2 in gas and aqueous phase (Figure 8) were fully optimized using DFT based on Beck's three parameter exchange functional and Lee–Yang–Parr nonlocal correlation functional (B3LYP) [10] and the 6–31G. The optimized molecular and selected angles, dihedral angles and bond lengths of P2 are given in figure 8. The optimized structure shows that the molecule P2 and have a non-planar structure. The HOMO and LUMO electrons density distributions of **P2** are given in Table 5.

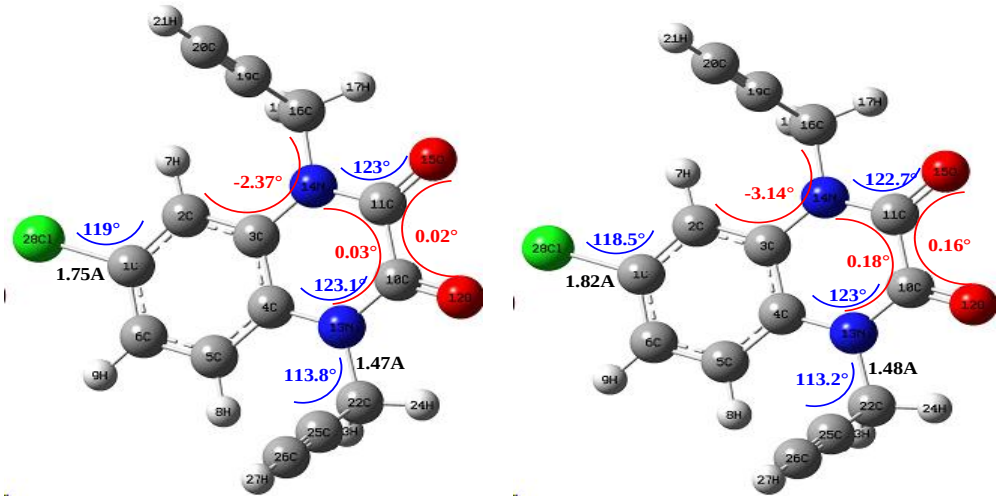

(P2) Gas phase (P2) Aqueous phase

Figure 8. Optimized molecular structures and selected dihedral angles (red), angles (blue) and bond lengths (black) of the studied inhibitors calculated in gas and aqueous phase with the DFT at the B3LYP/6-31G level.

After the analysis of the theoretical results obtained, we can say that the molecule **P2** have a non-planar structure.

Table 5. *The HOMO and the LUMO electrons density distributions of the studied inhibitors computed at B3LYP/6-31G level in gas and aqueous phases.*

	P2 Gas phase	**P2** Aqueous phase
HOMO	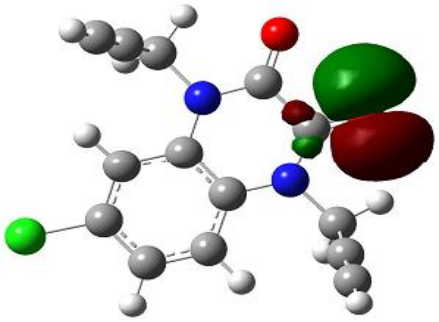	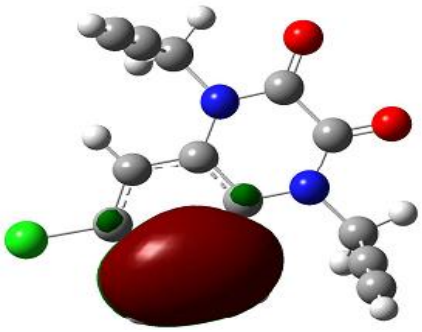
LUMO	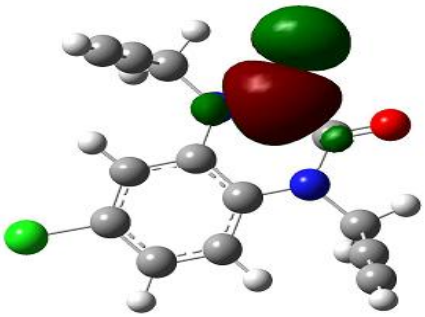	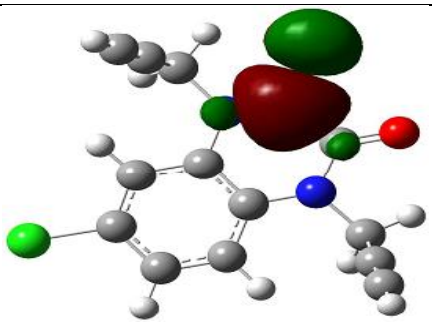

The inhibition efficiency afforded by the quinoline derivative P2 may be attributed to the presence of electron rich O.

Conclusion

Quinoxalines derivatives can be considered as effective corrosion inhibitors for the corrosion of the mild steel in 1M HCl solution. The molecules behave like mist type inhibitors. A corrosion inhibition efficiency of about 90% was recorded in the presence of 10^{-3} M of 6-chloroquinoxaline-2,3(1H,4H)-dione (P2) in 1 M HCl solutions. The corrosion inhibition was attributed to the adsorption of the inhibitor molecules through the oxygen atom and/or the nitrogen atom on the active corrosion centers of the electrode surface forming a blocking barrier to the corrosion process. The adsorption mode obeys the Langmuir adsorption isotherm and the calculated free energy of adsorption of both inhibitors on mild steel is in the range of –40.22 kJ mol^{-1} which reveals chemical adsorption. Quantum chemical studies and parameter values support the experimental results.

Reference

1. Elkacimi Y., Achnin M., Aouine Y., Ebn Touhami M., Alami A., Touir R., Sfaira M., Chebabe D., Elachqar A., Hammouti B., *Portugaliae Electrochimica Acta,* 30 (2012)53.
2. Elayyachy M., El Idrissi A., Hammouti B., *Corros. Sci* ,48 (2006) 2470.
3. Finšgar M., Jackson J., *Corros. Sci*. 86 (2014) 17.
4. Herrag L., Hammouti B., Elkadiri S., Aouniti A., Jama C., Vezin H., Bentiss F., *Corros. Sci.*, 52 (2010) 3042.
5. Dahmani M., Et-Touhami A., Al-Deyab S.S., Hammouti B., Bouyanzer A., *Int. J. Electrochem. Sci.*, 5 (2010) 1060.
6. Ibrahim M.A.M., Messali M., Moussa Z., Alzahrani A.Y., Alamry S.N., Hammouti B., *Electrochim. Acta*. 29

(2011) 375–389.
7. Lebrini M., Bentiss F., Vezin H., Lagren´ee M.,*Corros. Sci.*, 48 (2006) 1279.
8. El-Etre A.Y., Abdallah M., El-Tantawy Z.E., *Corros. Sci.*, 47 (2005) 389.
9. Verma C., Ebenso EE., Bahadur I., Obot IB., Quraishi MA. ; *Journal of Molecular Liquids* . 212(2015) 209-218.
10. Zarrouk A., Messali M., Zarrok H., Salghi R., Al-Sheikh Ali A ., Hammouti B., Al-Deyab S.S., Bentiss F., *J.Electrochem. Sci*. 7(2012) 6998–7015.
11. Dirlam J. P, Presslitz J. E., *Journal of Med. Chem*. 21(1978)483-48.
12. Ki Y.B, Kim Y.H., Park J.Y., Kim S.K., *Bio org. Med. Chem. Lett*.14(2004)541- 544.
13. Aguirre G., Cerecetto H., Di Maio R., Gonzalez M., Alfaro M.E.M., Jaso A., Zarranz B., Ortega M.A., Aldana I., Monge-Vega A., *Bioorg. Med. Chem. Lett*. 14(2004)3835-3839.
14. Elmsellem H., Aouniti A., Toubi Y., Steli H., Elazzouzi M., Radi S., Elmahi B., El Ouadi Y., Chetouani A., Hammouti B., *Der Pharma Chemica*. 7(7)(2015)353-364.
15. Elmsellem H., Bendaha H., Aouniti A., Chetouani A., Mimouni M., Bouyanzer A., *Mor. J. Chem*. 2 (1)(2014)1-9.
16. Hjouji M. Y., Djedid M., Elmsellem H., Kandri Rodi Y., Benalia M., Steli H., Ouzidan Y., Ouazzani Chahdi F., Essassi E. M., Hammouti B., *Der Pharma Chemica*. 8(4)(2016)85-95.
17. Essaghouani A. L., Elmsellem H., Ellouz M., El Hafi M., Boulhaoua M., Sebbar N. K., Essassi E. M., Bouabdellaoui M., Aouniti A. and Hammouti B., *Der Pharma Chemica*. 8(2) (2016)297-305.
18. Chakib I., Elmsellem H., Sebbar N. K., Lahmidi S., Nadeem A., Essassi E. M., Ouzidan Y., Abdel-Rahman I., Bentiss F., Hammouti B., *J. Mater. Environ. Sci*. 7(6)(2016)1866-1881.
19. Al Mamari Kh, Elmsellem H, Sebbar N.K., Elyoussfi A., Steli H., Ellouz M., Y. Ouzidan Y., Nadeem A., Essassi E.M., and El-Hajjaji F., *J. Mater. Environ. Sci*. 7(9) (2016) 3286-3299
10. Elmsellem H., Elyoussfi A., Sebbar N. K., Dafali A., Cherrak K., Steli H., Essassi E. M., Aouniti A. and Hammouti B., *Maghr. J. Pure & Appl. Sci*.1(2015)1-10.
21. Elmsellem H., Aouniti A.,Khoutoul M., Chetouani A., Hammouti B., Benchat N., Touzani R. and Elazzouzi M., *J. Chem. Pharm. Res*. 6(2014)1216.
22. Pearson R.G., *Inorg. Chem*. 27(1988) 734-740.
23. Sastri V.S., Perumareddi J.R., *Corrosion*. 53 (1997) 617-622.
24. Elmsellem H., Nacer H., Halaimia F., Aouniti A., Lakehal I., Chetouani A., Al-Deyab S. S., Warad I., Touzani R., Hammouti B, *Int. J. Electrochem. Sci*. 9(2014)5328.
25. Elmsellem H., Basbas N., Chetouani A., Aouniti A., Radi S., Messali M., Hammouti B., *Portugaliae. Electrochimica. Acta*. 2(2014)77.
26. Udhayakala P., Rajendiran T. V., Gunasekaran S., *Chem. J.Biol. Phys. SCI.A.* 2(3) (2012)1151-1165.
27. Ellouz M., Elmsellem H., Sebbar N. K., Steli H., Al Mamari K., Nadeem A., Ouzidan Y., Essassi E. M., Abdel-Rahaman I., Hristov P., *J. Mater. Environ. Sci*. 7(7) (2016)2482-2497.
28. Sikine M., Kandri Rodi Y., Elmsellem H., Krim O., Steli H., Ouzidan Y., Kandri Rodi A., Ouazzani Chahdi F., Sebbar N. K., Essassi E. M., *J. Mater. Environ. Sci*. 7(4) (2016)1386-1395.
29. Elmsellem H., Youssouf M. H., Aouniti A., Ben Hadd T., Chetouani A., Hammouti B., *Russian, Journal of Applied Chemistry*. 87(6) (2014) 744.
30. Elmsellem H., Harit T., AounitiA., Malek F., Riahi A., Chetouani A., Hammouti B., *Protection of Metals and Physical. Chemistry of Surfaces.* 51(5) (2015) 873.
31. Hjouji M. Y., Djedid M., Elmsellem H., Kandri Rodi Y., Ouzidan Y., Ouazzani Chahdi F., Sebbar N. K., Essassi E. M., Abdel-Rahman I., Hammouti B., *J. Mater. Environ. Sci*.7(4)(2016)1425-1435.
32. Popova A., Christov M., Raicheva S., Sokolova E., *Corros Sci*. 46 (2004) 1333–1350.
33. El Azzouzi M., Aouniti A., Tighadouin S., Elmsellem H., Radi S., Hammouti B., El Assyry A., Bentiss F., Zarrouk A., (2016). DOI: 10.1016/j.molliq.2016.06.007
34. Lipkowski J., Ross P.N. (Eds.), *Adsorption of Molecules at Metal Electrodes, VCH, New York*. (1992).
35. Elmsellem H., Elyoussfi A., Steli H., Sebbar N. K., Essassi E. M., Dahmani M., El Ouadi Y., Aouniti A., El Mahi B., Hammouti B., *Der. Pharma. Chemica*. 8(1)(2016) 248-256.
36. Elmsellem H., AounitiA., Youssoufi M.H., BendahaH., Ben hadda T., Chetouani A., Warad I., Hammouti B., *Phys. Chem. News*. 70 (2013) 84.
37. Elmsellem H., Elyoussfi A., Steli H., Sebbar N. K., Essassi E. M., Dahmani M., El Ouadi Y., Aouniti A., El Mahi B., Hammouti B., *Der Pharma Chemica*. 8(1) (2016) 248.

38. Aouniti A., Elmsellem H., Tighadouini S., Elazzouzi M., Radi S., Chetouani A., Hammouti B., Zarrouk A., *Journal of Taibah University for Science*. (2015). http://dx.doi.org/10.1016/j.jtusci.2015.11.008.
39. Sebbar N. K., Elmsellem H., Boudalia M., lahmidi S., Belleaouchou A., Guenbour A., Essassi E. M., Steli H., Aouniti A., *J. Mater. Environ. Sci*. 6 (11)(2015)3034-3044.
40. Filali Baba Y., Elmsellem H., Kandri Rodi Y., Steli H., AD C., Ouzidan Y., Ouazzani Chahdi F., Sebbar N. K., Essassi E. M., Hammouti B., *Der Pharma Chemica*. 8(4)(2016)159-169.
41. Riggs Jr. O.L., *Corrosion Inhibition, second ed., C.C. Nathan. Houston.TX*.(1973).
42. Ghareba S., Omanovic S., *Corros. Sci.* 52 (2010) 2104.
43. Gerengi H., Darowicki K., Bereket G., Slepski P., *Corros. Sci.* 51 (2009) 2573.
44. Brug G.J., Van DenEeden A.L.G., Sluyters-Rehbach M., SluytersJ.H., *J. Electroanal. Chem.*, 176 (1984) 275.
45. Moradi M., Duan J., Du X., *Corros. Sci.* 69(2013)338.
46. Tang Y., Zhang F., Huc S., Cao Z., Wu Z., Jing W., *Corros. Sci.*74(2013)271.
47. Schultze J.W., Wippermann K., *Electrochim. Acta.* 32(1987)823.
48. Martinez S., Metikos M., Hukovic, *J. Appl. Electrochem.*33(2003)137.
49. Hsu C.H., Mansfeld F., *Corrosion.* 57(2001)747.
50. Khamis E., *Corrosion.* 46(1990)6.
51. Chakib I., Elmsellem H., Sebbar N. K., Essassi E. M., Fichtali I., Zerzouf A., Ouzidan Y., Aouniti A., El Mahi B. and Hammouti B., *Der Pharma Chemica.* 8(2) (2016)380-391.
52. Elmsellem H., Elyoussfi A., Steli H., Sebbar N. K., Essassi E. M., Dahmani M., El Ouadi Y., Aouniti A., El Mahi B., Hammouti B., *Der. Pharma. Chemica*. 8(1)(2016) 248-256
53. Govindarajan M., Karabacak M., *Spectrochim Acta Part A Mol Biomol Spectrosc*. 85(2012)251–260.
54. K.F. Khaled, N.S. Abdelshafi, A. El-Maghraby, N. Al-Mobarak, *J. Mater. Environ. Sci*. 2(2011)166.
55. K. Ramji, D.R. Cairns, S. Rajeswari, *Appl. Surf. Sci*. 254 (2008) 4483–4493.
56. Elyoussfi A., Elmsellem H., Dafali A., Cherrak K., Sebbar N. K., Zarrouk A., Essassi E. M., Aouniti A., El Mahi B., Hammouti B., *Der Pharma Chemica*. 7(10) (2015) 284-291.
57. Lukovits I., Kalman E., Zucchi F., *Corrosion*, 57 (2001) 3-7.
58. Elmsellem H., Karrouchi K., Aouniti A., Hammouti B., Radi S., Taoufik J., Ansar M., Dahmani M., Steli H., El Mahi B., *Der Pharma Chemica*, 7(10) (2015) 237-245.

(2016) ; http://www.jmaterenvironsci.com/